Journal of Applied Mechanics and Technical Physics, Vol. 42, No. 6, pp. 972–978, 2001

EFFECT OF FREE-STREAM TURBULENCE ON THE BOUNDARY-LAYER STRUCTURE WITH DIFFUSION COMBUSTION OF ETHANOL

B. F. Boyarshinov and V. I. Titkov

UDC 536.244

The effect of turbulization of a subsonic air flow on the boundary-layer structure was experimentally studied during evaporation and combustion of ethanol behind an obstacle 3–6 mm *high. It is shown that turbulization increases the thermal boundary-layer thickness by a factor of* 2*, whereas the dynamic boundary-layer thickness changes weakly. For* 1–18% *turbulence at the entrance, the change in the momentum thickness along the channel is close to the change in the momentum thickness for a laminar isothermal boundary layer without injection. Local regions of elevated turbulence with a high intensity of heat and mass transfer arise in the case of combustion behind the obstacle at a distance of* 40–50 *obstacle heights.*

In real gas flows, the level of turbulence is usually high. For instance, we have $\mathrm{Tu}_0 = 2$–20% at the entrance to a gas turbine [1]. At a considerable part of turbine-blade surfaces (50–80%) exposed to combustion products, the boundary layer is in the state of laminar–turbulent transition, which occurs without the formation of instability waves and with closed separation [2]. The effect of the separation region on the flow structure and also on heat and mass transfer under conditions close to isothermal ones was studied in [3, 4]. At the reattachment point located at a distance of 10–18 heights h from the obstacle, friction stress changes its direction, turbulence and intensity of transfer processes increase, and inrush of the liquid to the wall and its outbursts into the main flow are observed. During combustion, flow reattachment is observed at a distance of $(6$–$9)h$ [5]. In the region of relaxation, heat and mass transfer exhibits properties of a laminar flow [6]. In this region, despite the elevated turbulence of the main flow ($\mathrm{Tu}_0 \approx 18\%$), the dependence between the Stanton (St) and Reynolds (Re) criteria has the form $\mathrm{St} \sim A\mathrm{Re}^{-0.5}$. A tendency to stratification of the measurement results is observed in experiments: within the measurement error of $\pm 15\%$, the coefficient A increases by an integer factor. This feature is not related to combustion.

With turbulization of the flow core, the separation region decreases, and the crossflow scales increase though to different extents: the thermal boundary layer becomes thicker than the dynamic one. The momentum thickness δ^{**}, which determines friction in the case without injection and streamwise pressure gradient, remained almost unchanged at a distance of 0.65 m in the experiments of [7]: $d\delta^{**}/dx \approx 0$. It was also noted that $d\delta^{**}/dx < 0$ in the region of "turbulence decay," where the values of $|d\mathrm{Tu}_0/dx|$ are maximum. The intensity of heat and mass transfer and friction in a nonreacting boundary layer depends not only on the level of turbulence but also on its spatial scale and generally increases with increasing Tu_0.

Obviously, the structure of the reacting boundary layer is a result of interaction of turbulence and combustion. In experiments with a plume [8], possible deceleration of mixing due to laminarization and, vice versa, additional turbulization in the boundary layer upon interaction of gases of different densities were noted. Turbulence increased monotonically along the channel near the wall but remained constant in the flow core [9]. In the experiments of [6], the effect of gas dynamics on combustion was manifested in the form of flameout.

Uncertainty of evaluation of each factor (separation, laminar–turbulent transition, and combustion) hinders mathematical simulation of their joint effect on gas-dynamic and thermal characteristics of the boundary layer. These characteristics may be most reliably determined experimentally. The available data are insufficient for

Kutateladze Institute of Thermal Physics, Siberian Division, Russian Academy of Sciences, Novosibirsk 630090. Translated from Prikladnaya Mekhanika i Tekhnicheskaya Fizika, Vol. 42, No. 6, pp. 55–63, November–December, 2001. Original article submitted May 16, 2001.

 0021-8944/01/4206-0972 $25.00

analysis of relations between the flow parameters and transfer processes in a turbulized reacting gas flow with a separation region. The objective of the present work is an experimental investigation of the boundary-layer structure with combustion for different levels of free-stream turbulence and also a comparison of the fields of temperature, velocity, and its fluctuations with the data on heat and mass transfer.

Experimental Setup and Measurement Technique. The experiments were performed in a wind tunnel, where a wire net with a 1×1 mm cell or a grid with 25 threading holes M27$\times$1.5 was placed at the confuser entrance. The confuser was attached to the test section 100×100 mm. The upper wall of the channel was absent, and the transparent side walls were made from a set of expandable quartz plates 65 mm wide. An obstacle of variable height $h = 3$–6 mm extended entrance over the entire channel width at the test-section entrance; upstream of the obstacle, there was a 8-mm slot for boundary-layer bleeding. The velocity of air removed through the slot was estimated as 10 m/sec. The turbulence at the test-section entrance ($\mathrm{Tu}_0 = 8$ or 18%) was controlled by the number of open holes in the grid (25 or 9). In experiments with the net, the value of Tu_0 depended on the method of introduction of dust particles into the flow in laser Doppler measurements: $\mathrm{Tu}_0 = 1\%$ if the particles were introduced only into the near-wall region and $\mathrm{Tu}_0 = 2.7\%$ if they were introduced into the main flow. According to [6], the rate of turbulence degeneration $d\mathrm{Tu}_0/dx$ increases with increasing Tu_0.

The streamwise velocity was measured by a laser Doppler anemometer. Quartz particles approximately 1 μm in diameter were used as scattering centers. The particles were located in a vessel shaken by a vibrator. The particles caught by air were introduced into the entrance cross section of the confuser either directly behind the grid or net through two tubes located between the holes [the inner diameter of the tubes was 10 mm and the flow rate of air (carrier of particles) was about 1 g/sec] or through a 0.8-cm^2 slot in the obstacle. In this case, the flow rate of air was approximately $4.2 \cdot 10^{-3}$ g/sec. The lower porous surface was formed by five square (80×80 mm) trays filled up to the brim by glass balls of diameter (0.7 ± 0.15) mm. The packing (it thickness was 8 mm) was replaced as it became contaminated by dust particles.

The velocity of the turbulized air flow U_0 was determined by the pressure difference in the flowmeter washer. The test liquid was 96% ethanol. The injection system ensured a constant content of ethanol in the packing, and the balls remained wet during the experiments. The ethanol evaporation rate from each element of the porous wall was self-established in accordance with the conditions of convective mass transfer and was close to values obtained in experiments with porous plates [6]. The free-stream temperature was $T_0 = 290$ K. The boundary-layer temperature was measured in the mid-plane of the test section by a platinum–(platinum–rhodium) thermocouple. The thermocouple electrodes 50 μm in diameter were butt-welded and stretched between ceramic tubes parallel to the porous plane (the outer diameter of the tubes was 0.5 mm, and the distance between them was 6 mm). The range of probe motion was 0–520 mm in the streamwise direction and 0–50 mm in the crossflow direction (with an accuracy of 0.1 mm).

The optical system of the LADO-2 anemometer [10] and the source of radiation (an LG-79-1 He–Ne laser of power 15 mW) were located at the platform of the traversing gear above the test section and were blown off by pure air. The range of streamwise motion was 0–400 mm (accuracy $\pm$0.5 mm), and the range of crossflow motion was 0–30 mm (accuracy $\pm$0.2 mm). An acoustooptical cell divided the laser beam ($\lambda = 632.8$ nm) into two parts in the plane parallel to the porous surface. The frequency difference between them was 20 MHz. Beams of approximate power of 3 mW were focused in the region of intersection of volume $0.1 \times 0.1 \times 0.5$ mm and entered the test section through a slot approximately 10 mm wide between the separated quartz plates of the side wall. Radiation scattered on particles was removed from the channel through a similar slot on the opposite wall and was registered by a photomultiplier. The signal proportional to the Doppler frequency shift, i.e., to the particle velocity, was identified using a processor [11], which was a tracking filter. The equipment allowed also the control over the number of particles passing through the measurement volume and the shape of the signal $U(t)$.

The use of a tracking filter has some special features, which were taken into account in conducting measurements. In particular, the obtained values of the mean velocity do not depend on the concentration of particles, level of turbulence, and signal-to-noise ratio, but one has to determine these parameters in measuring mean-velocity fluctuations u' and also to know the response time of the equipment and the degree of signal filtration, which is determined by the upper boundary of the frequency of flow-velocity oscillations. Therefore, the accuracy of determining $(u')^2$ in experiments was established by comparison with hot-wire results. In preliminary experiments without combustion in a flow powdered by 1-μm glycerine aerosol and quartz powder, it was found that in both cases the spectra of longitudinal velocity fluctuations within the range of 0–5 kHz and also the level of turbulence and the mean velocity coincide with each other and with hot-wire data, if the response time of the equipment is minimum

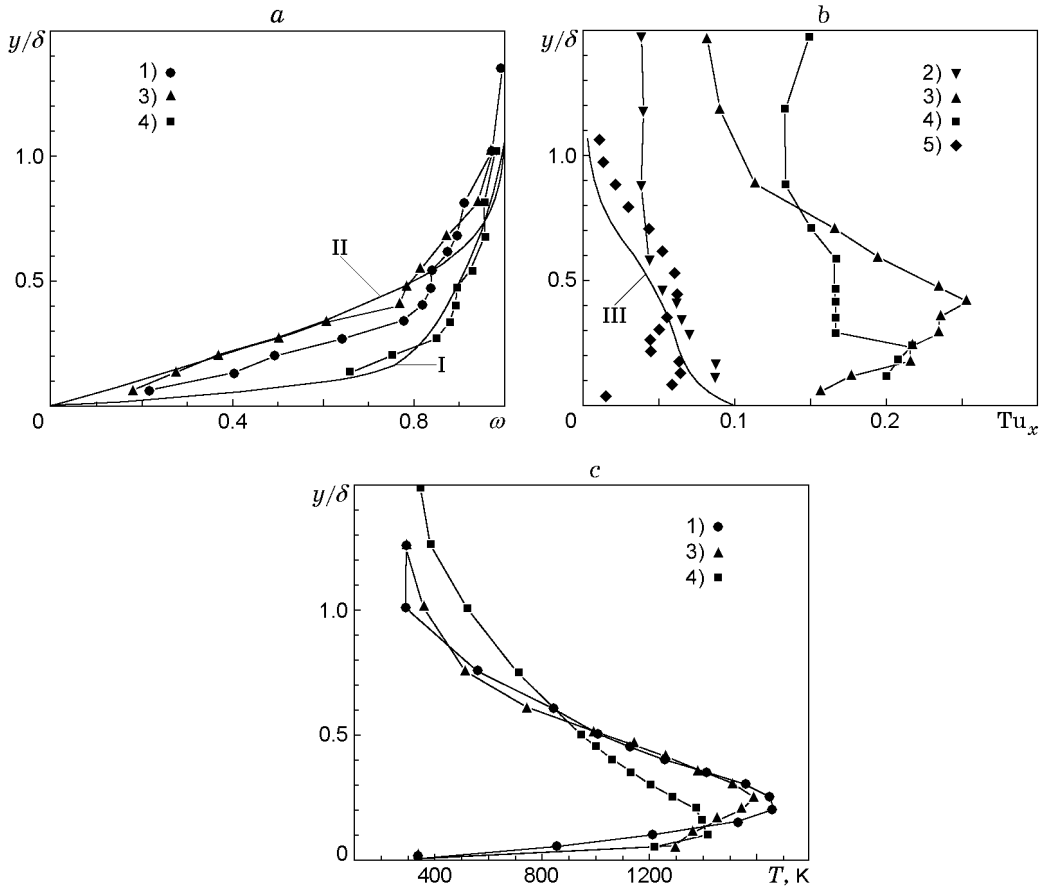

Fig. 1. Profiles of the streamwise mean (a) and fluctuating (b) velocities and mean temperature (c) in a turbulized boundary layer for evaporation and combustion of ethanol (h = 3 mm, U_0 = 10 m/sec, and x = 140 mm) for Tu_0 = 1 (points 1), 2.7 (points 2), 8 (points 3), and 18% (points 4); points 5 refer to the data of [9] for x = 120 mm; curve I refers to $\omega = U/U_0 = (y/\delta)^{1/7}$, curve II refers to the Blasius profile, and curve III refers to Klebanov's data [12].

and the number concentration of particles flying over the control volume is approximately 10^3 sec^{-1}. In the case of combustion, the signal-to-noise ratio decreases, and the threshold values of the signal are increased to ensure stable operation of the equipment, i.e., the number concentration of particles and the measured level of turbulence are artificially reduced to a certain level. The value of $(u')^2$ was corrected until the measured level of turbulence at the channel entrance coincided with the hot-wire data. It was assumed that only the intensity of velocity fluctuations changes at different points. In our estimates, this leads to an increase in the error of Tu determination up to ±20% but does not affect the final results, which depend on the unchanged tuning of the tracking filter: constant response time, degree of signal filtration, and number concentration of particles.

Test Results and Discussion. The research was performed for U_0 = 10 m/sec, h = 3 mm, and turbulence at the channel entrance Tu_0 = 1, 2.7, 8, and 18%. Under these conditions, the data were obtained for two cases: in the boundary layer on a smooth impermeable plate and for evaporation and combustion of ethanol above the porous surface. For Tu_0 = 8% (the turbulence at the flow centerline varies along the channel within 6–10%), additional experiments for h = 6 mm (U_0 = 10 m/sec) and also measurements at a distance z = 24 mm from the mid-plane for h = 3 mm for flow velocities U_0 = 10, 15, and 20 m/sec were performed. The minimum step in the streamwise direction for temperature and velocity profiles was Δx = 32.5 mm.

Some initial data typical of a turbulized boundary layer with combustion are plotted in Fig. 1 [δ = 15 mm is the distance from the wall, where $(U_0 - U)/U_0 = 0.01$, which corresponds to the measurement error]. Under conditions of the present experiments, the dynamic boundary-layer thickness varies little. The mean-velocity gradient on the wall $(\Delta U/\Delta y)_w$ may not only increase but also decrease with increasing free-stream turbulence. The shape

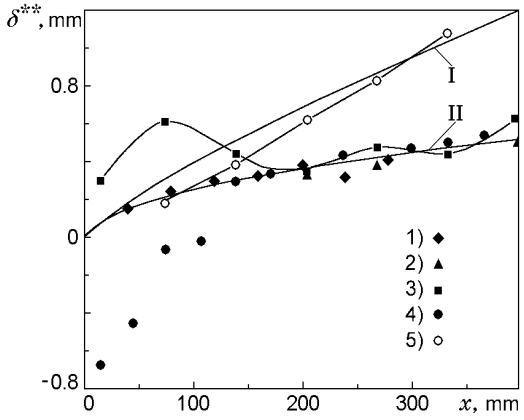

Fig. 2. Momentum thickness along the turbulized boundary layer in experiments with evaporation and combustion of ethanol (points 1–4) and without combustion (points 5) for $\mathrm{Tu}_0 = 1\%$ and $h = 3$ mm (1), $\mathrm{Tu}_0 = 8\%$ and $h = 3$ mm (2), $\mathrm{Tu}_0 = 18\%$ and $h = 3$ mm (3), and $\mathrm{Tu}_0 = 8\%$ and $h = 6$ (4); curve I refers to the dependence $\delta^{**}(x)$ for a standard turbulent boundary layer and curve II refers to $\delta^{**} = 0.664(\nu x/U_0)^{0.5}$.

of the profiles varies within wide limits approaching experimental data both for turbulent $\omega = U/U_0 = (y/\delta)^{1/7}$ (curve I) and laminar (curve II) boundary layers.

Figure 1b shows that the level of boundary-layer turbulence drastically increases with increasing Tu_0. For $\mathrm{Tu}_0 = 2.7\%$, it is close to the level of turbulence in the case without combustion (curve III), and the greatest values are reached for $\mathrm{Tu}_0 = 8\%$. The maximum value $\mathrm{Tu}_{\max} \approx 25\%$ is observed far from the wall, which is typical of the laminar–turbulent transition regime. The data of [9] correspond to injection of the $H_2 + N_2$ mixture and its combustion in air ($U_0 = 10$ m/sec and $\mathrm{Tu}_0 = 0.7\%$) under conditions where the dynamic boundary layer is developed upstream and is thicker than the thermal boundary layer ($x_0 = -1$ m and $\delta = 40$ mm).

Deformation of temperature profiles is shown in Fig. 1c. With increasing Tu_0, the maximum values of T decrease and are shifted toward the wall. The thermal boundary-layer thickness δ_t (the ordinate of the temperature-profile point with $T = 300$ K) may be twice the dynamic boundary-layer thickness δ. The reason seems to be the difference in density of the interacting flows. Portions of the cold gas from the main flow penetrate deeper into the near-wall region and, interacting with high-temperature combustion products, cause outbursts of large volumes of the heated gas into the outer part of the boundary layer. The difference in density may be also the reason for strong turbulization (see Fig. 1b).

The data obtained allow us to determine the integral scales of the turbulized boundary layer under conditions of combustion. The displacement thickness $\delta^* = \int_0^{\delta_t} (1 - (\rho/\rho_0)\omega)\, dy$ increases by a factor of 1.5–2 due to turbulization and may exceed the corresponding value for a standard boundary layer (isothermal flow past a smooth impermeable wall) by more than a factor of 20. Figure 2 shows the distribution of the momentum thickness $\delta^{**} = \int_0^{\delta} (\rho/\rho_0)\omega(1-\omega)\, dy = \delta_0^{**} + \delta^{**}(x)$ along the channel in experiments with and without combustion. In this case, the data obtained are shifted along the ordinate axis by a constant value δ_0^{**}. In experiments without combustion, we have $\delta_0^{**} = 0.7$ mm, and the derivative $d\delta^{**}/dx$ is slightly higher than the corresponding value for a standard turbulent flow (curve I), which is in agreement with the known data on increasing friction in an isothermal turbulized boundary layer. In combustion (points 1–4), for all values of Tu_0, the results for $\delta^{**}(x)$ measured for $x > 200$ mm are close to the values of δ^{**} for a laminar isothermal boundary layer without injection: $\delta^{**} = 0.664(\nu x/U_0)^{0.5}$ (curve II). For a high initial level of turbulence ($\mathrm{Tu}_0 = 18\%$), the momentum thickness decreases at the section $x = 75$–205 mm, which was also noted in experiments without combustion.

Analyzing the possibility of existence of the relation $d\delta^{**}/dx < 0$ for a nonreacting boundary layer, Ames and Moffat [13] did not arrive at a definite conclusion, since the longitudinal pressure gradient was not known. Using the same approach as in [13] (integration of the Reynolds equations for a two-dimensional case, where the

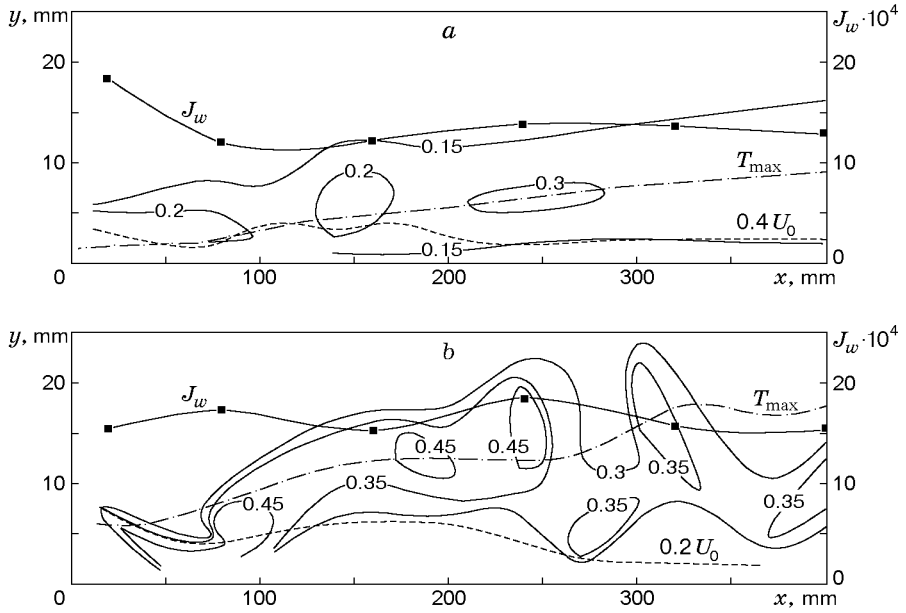

Fig. 3. Isolines of turbulence (solid curves) and mean velocity (dashed curve), isotherm $T_{\max}$ (dot-and-dashed curve), and dimensionless burning rate for ethanol [6] (points) in a turbulized boundary layer for $U_0 = 10$ m/sec, $\mathrm{Tu}_0 = 8\%$ and $h = 3$ (a) and 6 mm (b).

second equation has the form $\partial P/\partial y = -\rho\partial\nu'^2/\partial y)$, we obtain the momentum integral equation for a turbulent reacting boundary layer:

$$\frac{d(\delta^{**} - \Delta)}{dx} + [2(\delta^{**} - \Delta) + \delta^*]\,\frac{1}{U_0}\,\frac{dU_0}{dx} = \frac{C_F}{2} + J. \tag{1}$$

Here the effect of turbulization here is taken into account through the anisotropy thickness

$$\Delta = \int_0^S \frac{\rho}{\rho_0}(\mathrm{Tu}_x^2 - \mathrm{Tu}_y^2)\,dy$$

(Tu_x and Tu_y are the streamwise and crossflow levels of turbulence; integration is performed in the region $0 < y < S$, where $\mathrm{Tu}_x \neq \mathrm{Tu}_y$), $C_F/2$ is the friction coefficient, and $J = \rho_w v_w/(\rho_0 U_0)$ is the relative flux of the substance injected from the wall.

In the case considered, we have $dU_0/dx = 0$ and $J = 0$. The right part of the momentum equation is positive and weakly depends on variation of the ambient conditions [14]. Therefore, for $d\delta^{**}/dx < 0$, Eq. (1) is valid if $\Delta > \delta^{**}$ and $d\Delta/dx < 0$, i.e., for a high rate of degeneration of free-stream turbulence, when $\mathrm{Tu}_x > \mathrm{Tu}_y$ and $d\mathrm{Tu}_0/dx < 0$. The quantity Tu_y was not measured, and the ratio Δ/δ^{**} is not known. For a standard nonreacting boundary layer, we have $\Delta/\delta^{**} = 1.42 \cdot 10^{-2}$ [12]. For $\mathrm{Tu}_0 = 18\%$, the estimates yield $d\delta^{**}/dx \approx d\Delta/dx$ near the channel entrance, and the relation $d\delta^{**}/dx < 0$ is valid. Nevertheless, for a reliable analysis of Eq. (1), one should determine the fields $\mathrm{Tu}_x(x, y)$ and $\mathrm{Tu}_y(x, y)$.

It follows from experimental data that local longitudinal gradients of turbulence in the boundary layer may be located far from the obstacle. Figure 3a shows that there are three local regions of elevated turbulence in the boundary layer (two regions for $\mathrm{Tu}_0 = 2.7\%$), which correspond to bends on the isotach $0.4U_0$. Their position is well visualized by sections of the porous surface with an elevated intensity of deposition of the powder used as dust for the main flow. This fact is manifested more clearly with increasing height of the obstacle. Isolines for $h = 6$ mm are shown in Fig. 3b. The number of regions of elevated turbulence has increased. Two of them are located in an immediate vicinity of the wall at distances $x/h = 10$–15 and $x/h \approx 45$. The isotach $0.2U_0$ is twice bent toward the wall; the relative burning rate $J_w = j_w/(\rho_0 U_0)$ near these regions increases. The above features are also observed in the cross section $z = 24$ mm. As the velocity increases, these regions are extended streamwise and are almost absent for $\mathrm{Tu}_0 = 18\%$. The error in determining their boundaries is $\Delta x/2 \approx 16$ mm in the streamwise direction and approximately 0.5 mm in the crossflow direction.

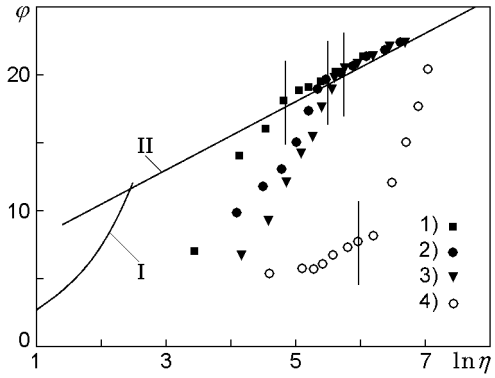

Fig. 4. Velocity profiles for combustion in the boundary layer (U_0 = 10 m/sec): points 1 refer to h = 3 mm, Tu_0 = 18%, and x = 140 mm, points 2 to h = 3 mm, Tu_0 = 18%, and x = 270 mm, points 3 to h = 3 mm, Tu_0 = 1%, and x = 270 mm, and points 4 to h = 6 mm, Tu_0 = 8%, and x = 270 mm (4); curves I and II refer to $\varphi = \eta$ and $\varphi = (1/\chi)\ln\eta + 5.5$, respectively.

Figure 4 shows the velocity profiles in the logarithmic coordinates $\varphi = \omega/(C_F/2)^{0.5}$ and $\eta = yU_0(C_F/2)^{0.5}/\nu$, where $C_F/2 = \mathrm{Sc}^{0.6}\mathrm{St}_d$, i.e., the analogy between friction and mass transfer is used. Here Sc is the Schmidt number and the values $\mathrm{St}_d = j_w/(\rho_0 U_0 C_w)$ are borrowed from [6] for the same test conditions as in the present work. A reverse flow was registered in experiments with combustion (U_0 = 10 m/sec, Tu_0 = 8%, and h = 6 mm) for $x < 50$ mm. The isotherm T = 1000 K intersect the region $U < 0$. In the remaining cases, the reverse flow was not found with distance from the obstacle. Two characteristic regions with $T = T_{\max}$ (vertical lines in Fig. 4) located above and below the coordinate $y = y_f$ are observed in the turbulent boundary-layer structure: 1) turbulent external part $y > y_f$ with a logarithmic section, where $\chi = 0.4$ (this section increases with increasing Tu_0 and is clearly manifested in experiments with Tu_0 = 18%); 2) internal part $y < y_f$, where the experimental data disagree with curve I, though as in the known cases of separated flows with and without combustion [4], they approach the numerical results for a laminar shear layer in the coordinates $\omega = f(y/\delta)$ (see Fig. 1a). In the case of strong separation (U_0 = 10 m/sec, Tu_0 = 8%, and h = 6 mm), the results are lower than curve II even for y = 30 mm.

Conclusions. The present study shows that turbulization has a strong effect on the boundary-layer structure with combustion. In experiments, turbulization was excited both in the main flow and in an immediate vicinity of the wall behind a variable-height obstacle. As in experiments without combustion, turbulization increases the thermal boundary-layer thickness, whereas the dynamic boundary-layer thickness changes weakly. For high levels of turbulence at the channel entrance and high values of its longitudinal gradient, the momentum thickness may decrease downstream. Experimental data tend to approach the numerical results for friction in a laminar boundary layer in the absence of turbulization, injection, and combustion for Tu_0 = 1–18% and h = 3–6 mm with distance from the entrance.

In the case of combustion, the difference in density of the interacting gases may lead to a significant increase in boundary-layer turbulence. Under test conditions for an obstacle of height h = 3 mm, a turbulent mechanism of momentum transfer is retained in the external region of the boundary layer up to the flame front. With increasing obstacle height (h = 6 mm), the flow-separation region is extended to the whole boundary layer.

Reattachment regions, where the transfer processes are drastically intensified, may appear if the intense rotational motion behind the obstacle at a distance of several height decays, and further flow development follows the laminar boundary-layer scenario. These processes may lead to some stratification in the measured characteristics of heat and mass transfer [15]. Indirect signs of flow reattachment may be local bends of equivelocity contours and the presence of elevated-turbulence regions of limited length and surface sections with elevated heat and mass transfer and the disperse phase leaving the flow. The existence of such large-scale stationary nonuniformities is important for constructing a physical model of a turbulized near-wall flow and for analysis of combustion processes in solid-fuel ramjets and other power-engineering facilities.

This work was supported by the Russian Foundation for Fundamental Research (Grant No. 99-02-17171).

REFERENCES

1. A. B. Turner, "Local heat transfer measurements on a gas turbine blade," *J. Mech. Eng. Sci.*, **13**, No. 1, 1–12 (1971).
2. E. P. Dyban, É. Ya. Épik, and L. E. Yushina, "Heat transfer on a streamwise plate with separation and turbulization of the external flow," *Prom. Teplotekh.*, **17**, Nos. 1/3, 3–12 (1995).
3. I. P. Castro and A. Haque, "The structure of shear layer bounding separation region. Part 2. Effects of free-stream turbulence," *J. Fluid Mech.*, **192**, 577–595 (1988).
4. J. K. Eaton and J. P. Johnston, "A review of research on subsonic turbulent flow reattachment," *AIAA J.*, **19**, No. 9, 1093–1100 (1981).
5. G. Schulte, "Fuel regression and flame stabilization studies of solid-fuel ramjets," *J. Propul. Power*, No. 4, 301–304 (1986).
6. B. F. Boyarshinov, Some characteristics of heat and mass transfer in a turbulent air flow over a surface," *Prikl. Mekh. Tekh. Fiz.*, **41**, No. 4, 124–130 (2000).
7. K. A. Thole and D. G. Bogard, "High free-stream turbulence effects on turbulent boundary layers," *Trans. ASME, J. Fluids Eng.*, **118**, 276–284 (1996).
8. Yu. Ya. Buriko and A. B. Lebedev, "Turbulent mixing and diffusion combustion of a jet in a channel," *Izv. Akad. Nauk SSSR, Mekh. Zhidk. Gaza*, No. 4, 25–33 (1980).
9. T. Ueda, M. Mizomoto, S. Ikai, and T. Kobayashi, "Velocity and temperature fluctuations in a flat plate boundary layer diffusion flame," *Combust. Sci. Technol.*, **27**, 133–142 (1982).
10. Yu. N. Dubnishchev and B. S. Rinkevichyus, *Methods of Laser Doppler Anemometry* [in Russian], Nauka, Moscow (1982).
11. V. I. Titkov and Ya. Ya. Tomsons, "Tracking filter-demodulator," USSR Author's Certificate No. 748799, MKI^2 H 03 D 13/00; G 01 S 9/24; H 03 B 3/04, No. 2565595/18-09; Appl. 01.05.78; Publ. 07.25.80, Bul. No. 26.
12. G. Schlichting, *Boundary Layer Theory*, McGraw-Hill, New York (1968).
13. F. E. Ames and R. J. Moffat, "Heat transfer with high intensity, large scale turbulence: the flat plate turbulent boundary layer and the cylindrical stagnation point," Report No. N HMT-44, Stanford Univ., Stanford, California (1990).
14. V. M. Ievlev, "Some issues of the hydrodynamic theory of heat transfer in a gas flow," *Dokl. Akad. Nauk SSSR*, **87**, 21–24 (1952).
15. B. F. Boyarshinov, "Analysis of experimental data on heat and mass transfer in a boundary layer," *Fiz. Goreniya Vzryva*, **34**, No. 2, 73–81 (1998).